arXiv:1409.2999v1 [hep-ph] 10 Sep 2014

Neutrino masses, dark matter and baryon asymmetry of the Universe

Amine Ahriche[(1)] **and Salah Nasri**[(2)]

[(1)] Department of Physics, University of Jijel, PB 98 Ouled Aissa, DZ-18000 Jijel, Algeria.
[(2)] Physics Department, UAE University, POB 17551, Al Ain, United Arab Emirates.

E-mail: aahriche@ictp.it, snasri@uaeu.ac.ae

Abstract. In this work, we try to explain the neutrino mass and mixing data radiatively at three-loop by extending the standard model (SM) with two charged singlet scalars and three right handed (RH) neutrinos. Here, the lightest RH neutrino is a dark matter candidate that gives a relic density in agreement with the recent Planck data, the model can be consistent with the neutrino oscillation data, lepton flavor violating processes, the electroweak phase transition can be strongly first order; and the charged scalars may enhance the branching ratio $h \to \gamma\gamma$, where as $h \to \gamma Z$ get can get few percent suppression. We also discuss the phenomenological implications of the RH neutrinos at the collider.

1. Introduction

The Standard Model (SM) of particle physics has been very successful in describing nature at the weak scale, however, there are many unexplained puzzles left, that implies going beyond SM. Three concrete evidences for Physics beyond SM are: (i) non zero neutrino masses, (ii) the existence of dark matter (DM), and (iii) the observation of matter anti matter asymmetry of the universe. However, most of the SM extensions make no attempt to address these three puzzles within the same framework. For instance, a popular extension of the SM, is introducing very heavy right-handed (RH) neutrinos ($m_N \geq 10^8$ GeV), where small neutrino masses are generated via the see-saw mechanism [1], and the BAU is produced via leptogenesis [2]. Unfortunately, a RH neutrino heavier than 10^7 GeV, decouples from the effective low energy theory, and can not be tested at collider experiments.

A small neutrino mass can be generated radiatively, where the famous example is the so-called Zee model [3]. In Zee-model, the solar mixing angle comes out to be close to maximal, which is excluded by the solar neutrino oscillation data [4]. This problem is circumvented in models where neutrinos are induced at two loops [5] or three loops [6, 7]. One of the advantages of this class of models is that all the mass scales are in the TeV or sub-TeV range, which makes it possible for them to be tested at future colliders. In Ref. [6], the SM was extended with two charged $SU(2)_L$ singlet scalars and one RH neutrino field, N, where a Z_2 symmetry was imposed to forbid the Dirac neutrino mass terms at tree level [6]. After the electroweak symmetry breaking, tiny neutrino masses are naturally generated at three loops due to the high loop suppression. A consequence of the Z_2 symmetry and the field content of the model, N is Z_2-odd, and thus guaranteed to be stable, which makes it a good DM candidate. In Ref. [8], the authors considered extending the fermion sector of the SM with two RH neutrinos, in order for

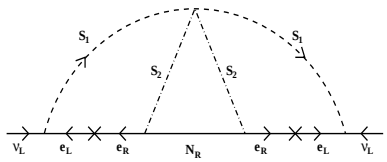

Figure 1. *The three-loop diagram that generates the neutrino mass.*

it to be consistent with the neutrino oscillation data, and they studied also its phenomenological implications.

In [9], we calculated the three loop neutrino masses exactly, as compared to the approximate expression derived in [6]. We have shown that in order to satisfy the recent experimental bound on the lepton flavor violating (LFV) process such as $\mu \to e\gamma$ [10]; and the anomalous magnetic moment of the muon [11], one must have three generations of RH neutrinos. Taking into account the neutrino oscillation data and the LFV constraints, we show that the lightest RH neutrino can account for the DM abundance with masses lighter than 225 GeV. The presence of the charged scalars in this model will affect the Higgs decay process $h \to \gamma\gamma$ and can lead to an enhancement with respect to the SM, where as $h \to \gamma Z$ is slightly reduced. In this model, we find that a strongly electroweak phase transition can be achieved with a Higgs mass of $\simeq 125$ GeV as measured at the LHC [12, 13].

This letter is organized as follows. In the next section we present the model, and discuss the constraints from the LFV processes. In section III, we study the relic density of the lightest RH neutrino and different DM features in this model. Section IV is devoted to the study of the electroweak phase transition combined with the effect of the presence of extra charged scalars on the Higgs decay channels $h \to \gamma\gamma$ and $h \to \gamma Z$. In section V, we discuss the phenomenological implications of the RH neutrinos at the ILC. Finally we conclude in section VI.

2. Neutrino Mass & Mixing

Our model is just the SM extended by three RH neutrinos, N_i, and two charged singlet scalars, $S_1^{\pm}$ and $S_2^{\pm}$. In addition, we impose a discrete Z_2 symmetry on the model, under which $\{S_2, N_i\} \to \{-S_2, -N_i\}$, and all other fields are even. The Lagrangian reads

$$\mathcal{L} = \mathcal{L}_{SM} + \{f_{\alpha\beta} L_\alpha^T C i\tau_2 L_\beta S_1^+ + g_{i\alpha} N_i S_2^+ \ell_{\alpha R} + \tfrac{1}{2} m_{N_i} N_i^C N_i + h.c\} - V(\Phi, S_1, S_2), \qquad (1)$$

where L_α is the left-handed lepton doublet, C is the charge conjugation matrix, $f_{\alpha\beta}$ are Yukawa couplings which are antisymmetric in the generation indices α and β, m_{N_i} are the Majorana RH neutrino masses; and $V(\Phi, S_1, S_2)$ is the tree-level scalar potential which is given by

$$\begin{aligned} V(\Phi, S_i) = \lambda \left(|\Phi|^2\right)^2 - \mu^2 |\Phi|^2 + \textstyle\sum_i \{m_i^2 S_i^* S_i + \lambda_i S_i^* S_i |\Phi|^2 + \frac{\eta_i}{2} (S_i^* S_i)^2\} \\ + \{\lambda_s S_1 S_1 S_2^* S_2^* + h.c\}, \end{aligned} \qquad (2)$$

where Φ is the SM Higgs doublet. The Z_2 symmetry imposed on the Lagrangian implies:
(1) if N_1 is the lightest particle among N_2, N_3, S_1 and S_2, then it would be stable, and hence it is a candidate for dark matter. Moreover, N_i will be pair produced and subsequently decay into N_1 (or to N_2 and then to N_1) and a pair (or two pairs) of charged leptons. We will discuss its phenomenology later. (2) The Dirac neutrino mass term is forbidden at all levels of the perturbation theory, and Majorana neutrinos masses are generated radiatively at three-loops, as shown in Fig. 1-left.

The exact estimation of the diagram in Fig. 1 leads to [9]

$$(M_\nu)_{\alpha\beta} = \frac{\lambda_s m_{\ell_i} m_{\ell_k}}{(4\pi^2)^3 m_{S_2}} f_{\alpha i} f_{\beta k} g_{ij} g_{kj} F\left(m_{N_j}^2/m_{S_2}^2, m_{S_1}^2/m_{S_2}^2\right), \qquad (3)$$

where $\rho, \kappa, j(i,k)$ are flavor (eigenstates) indices, and the function F is a loop integral given in (A.8) in [9], which was approximated to one in the original work [6]. In this model, the radiatively generated neutrino masses are directly proportional to the charged leptons and RH neutrino masses as shown in (3) unlike the conventional seesaw mechanism. The neutrino mass matrix elements (3) should fit the experimental values

$$(M_\nu)_{\alpha\beta} = [U \cdot diag(m_1, m_2, m_3) \cdot U^T]_{\alpha\beta}, \tag{4}$$

where U is the Pontecorvo-Maki-Nakawaga-Sakata (PMNS) mixing matrix [14], where the mixing angles are given by the experimental allowed values for $s^2_{12} = 0.320^{+0.016}_{-0.017}$, $s^2_{23} = 0.43^{+0.03}_{-0.03}$, $s^2_{13} = 0.025^{+0.003}_{-0.003}$, with $s_{ij} \equiv \sin(\theta_{ij})$ and $c_{ij} \equiv \cos(\theta_{ij})$, and the mass differences $\left|\Delta m^2_{31}\right| = 2.55^{+0.06}_{-0.09} \times 10^{-3}$ eV^2 and $\Delta m^2_{21} = 7.62^{+0.19}_{-0.19} \times 10^{-5}$eV^2 [15].

Besides neutrino masses and mixing, the Lagrangian (1) induces flavor violating processes such as $\ell_\alpha \to \gamma \ell_\beta$ if $m_{\ell_\alpha} > m_{\ell_\beta}$, generated at one loop via the exchange of both extra charged scalars $S_i^\pm$. The branching ratio of such process can be computed as [9]

$$B(\ell_\alpha \to \gamma \ell_\beta) = \frac{\alpha_{em} v^4}{384\pi} \left\{ \frac{\left| f_{\kappa\alpha} f^*_{\kappa\beta} \right|^2}{m^4_{S_1}} + \frac{36}{m^4_{S_2}} \left| \sum_i g_{i\alpha} g^*_{i\beta} F_2\left(\frac{m^2_{N_i}}{m^2_{S_2}}\right) \right|^2 \right\}, \tag{5}$$

with $\kappa \neq \alpha, \beta$, α_{em} is the fine structure constant and $F_2(x) = (1-6x+3x^2+2x^3-6x^2\ln x)/6(1-x)^4$. Another constraint which the bound on the muon anomalous magnetic moment δa_μ, that receives the contribution [9]

$$\delta a_\mu = \frac{m^2_\mu}{16\pi^2} \left\{ \frac{|f_{\mu e}|^2 + |f_{\mu\tau}|^2}{6 m^2_{S_1}} + \frac{1}{m^2_{S_2}} \sum_i |g_{i\mu}|^2 F_2\left(\frac{m^2_{N_i}}{m^2_{S_2}}\right) \right\}. \tag{6}$$

In Fig. 2-left, we show a scattered plot of the muon anomalous magnetic moment versus the $\beta\beta_{0\nu}$ decay effective Majorana mass $(M_\nu)_{ee}$, where the considered upper bound is $(M_\nu)_{ee} < 0.35$ eV [16]. In our parameter space scan, we consider $m_{S_{1,2}} \geq 100$ GeV**;** and demanded that (3) to be consistent with the neutrino oscillation data. From Fig. 2-left, one can see that most of the values of $(M_\nu)_{ee}$ that are consistent with the bound on δa_μ are lying in the range 10^{-3} eV to $\sim$eV.

Fig. 2-right gives an idea about the magnitude of the couplings that satisfy the constraints from LFV processes and the muon anomalous magnetic moment, and which also are consistent with the neutrino oscillation data. It is worth noting that when considering just two generations of RH neutrinos (i.e, $g_{3\alpha} = 0$), we find that the bound $B(\mu \to e\gamma) < 5.7 \times 10^{-13}$ is violated [10]. Therefore, having three RH neutrinos is necessary for it to be in agreement with the data from the bounds from LFV processes. Moreover, one has to mention that the bound on $B(\mu \to e\gamma)$ makes the parameters space very constrained. For instance, out of the benchmarks that are in agreement with the neutrino oscillation data, DM and δa_μ, only about 15% of the points will survive after imposing the $\mu \to e\gamma$ bound.

3. Dark Matter

As mentioned above, the lightest RH neutrino N_1 is stable, and could be the DM candidate. In the case of hierarchical RH neutrino mass spectrum, we can safely neglect the effect of N_2 and N_3 on N_1 density. The N_1 number density get depleted through the annihilation process $N_1 N_1 \to \ell_\alpha \ell_\beta$ via the t-channel exchange of $S_2^\pm$. After estimating the Feynman diagrams,

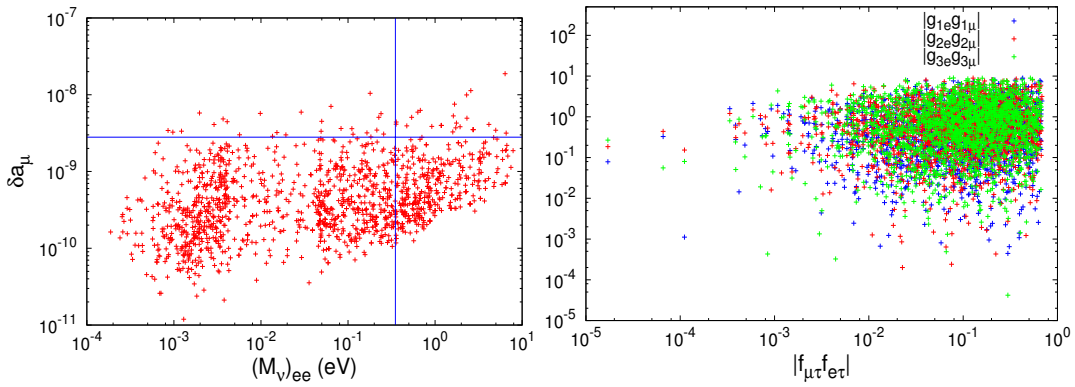

Figure 2. *Left: The muon anomalous magnetic moment versus the $\beta\beta_{0\nu}$ decay effective Majorana $(M_\nu)_{ee}$. The blue lines represent their experimental upper bounds. Right: Different parameters combinations (as absolute values) that are relevant to the LFV constrain on $B(\mu \to e\gamma)$, are shown where (3) and (4) are matched.*

squaring, summing and averaging over the spin states, we find that in the non-relativistic limit, the total annihilation cross section is given by

$$\sigma_{N_1 N_1} \upsilon_r \simeq \sum_{\alpha,\beta} |g_{1\alpha} g^*_{1\beta}|^2 \frac{m^2_{N_1}\left(m^4_{S_2} + m^4_{N_1}\right)}{48\pi\left(m^2_{S_2} + m^2_{N_1}\right)^4} \upsilon_r^2, \tag{7}$$

with υ_r is the relative velocity between the annihilation N_1's. As the temperature of the universe drops below the freeze-out temperature $T_f \sim m_{N_1}/25$, the annihilation rate becomes smaller than the expansion rate (the Hubble parameter) of the universe, and the N_1's start to decouple from the thermal bath. The relic density after the decoupling can be obtained by solving the Boltzmann equation, and it is approximately given by [9]

$$\Omega_{N_1} h^2 \simeq \frac{1.28 \times 10^{-2}}{\sum_{\alpha,\beta} |g_{1\alpha} g^*_{1\beta}|^2} \left(\frac{m_{N_1}}{135\ \text{GeV}}\right)^2 \frac{\left(1 + m^2_{S_2}/m^2_{N_1}\right)^4}{1 + m^4_{S_2}/m^4_{N_1}}, \tag{8}$$

In Fig. 3, we plot the allowed mass range (m_{N_1}, m_{S_i}) plane that give the observed dark matter relic density [17]. As seen in the figure, the neutrino experimental data combined with the relic density seems to prefer $m_{S_1} > m_{S_2}$ for large space of parameters. However, the masses of both the DM and the charged scalar $S_2^\pm$ can not exceed $m_{N_1} < 225$ GeV and $m_{S_2} < 245$ GeV, respectively.

In computing the relic density in (8), we have assumed that there is a hierarchy between the three right-handed neutrino masses. However, when the possibility for N_2 and/or N_3 being close in mass to N_1, i.e $\Delta_i = (m_{N_i} - m_{N_1})/m_{N_1} << 1$, is considered, the coannihilation processes like $N_1 N_{2,3} \to \ell_\alpha \ell_\beta$ might enhance the relic density values by three if the degeneracy is around $\Delta_2 \sim 0.1$.

4. Electroweak Phase Transition & Higgs Decay

It is well known that the SM has all the qualitative ingredients for electroweak baryogenesis, but the amount of matter-antimatter asymmetry generated is too small. One of the reasons is that the electroweak phase transition (EWPT) is not strongly first order, which is required to suppress the sphaleron processes in the broken phase. The strength of the EWPT can be

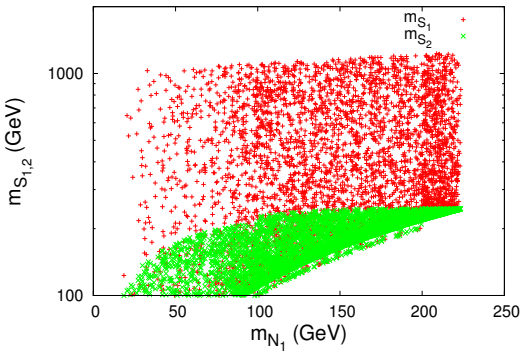

Figure 3. *The charged scalar masses m_{S_1} (red) and m_{S_2} (green) versus the lightest RH neutrino mass, where the consistency with the neutrino data, LFV constraints and the DM relic density have been imposed.*

improved if there are new scalar degrees of freedom around the electroweak scale coupled to the SM Higgs, which is the case in the model that we are considering in this paper.

The investigation of the transition dynamics and its strength requires the precise knowledge of the effective potential of the CP-even scalar fields at finite temperature [18]. The one-loop Higgs effective potential is given in the $\overline{DR}$ scheme by

$$V_{eff}(h,T) = \frac{\lambda}{4!}h^4 - \frac{\mu^2}{2}h^2 + \sum_i n_i \frac{m_i^4(h)}{64\pi^2}\left(\ln\left(\frac{m_i^2(h)}{\Lambda^2}\right) - \frac{3}{2}\right), \\ + \frac{T^4}{2\pi^2}\sum_i n_i J_{B,F}\left(m_i^2/T^2\right) + V_{ring}(h,T); \tag{9}$$

$$V_{ring}(h,T) = -\frac{T}{12\pi}\sum_i n_i \left\{\tilde{m}_i^3(h,T) - m_i^3(h)\right\}, \tag{10}$$

$$J_{B,F}(\alpha) = \int_0^\infty x^2 \log(1 \mp \exp(-\sqrt{x^2+\alpha})), \tag{11}$$

where $h = (\sqrt{2}Re(H^0) - v)$ is the real part of the neutral component in the doublet, n_i are the field multiplicities, $m_i^2(h)$ are the field-dependent mass squared which are given in Appendix B in [9], and Λ is the renormalization scale which we choose to be the top quark mass. where the summation is performed over the scalar longitudinal gauge degrees of freedom, and $\tilde{m}_i^2(h,T)$ are their thermal masses, which are given in Appendix B. The contribution (10) is obtained by performing the resummation of an infinite class of of infrared divergent multi-loops, known as the ring (or daisy) diagrams, which describes a dominant contribution of long distances and gives significant contribution when massless states appear in a system. It amounts to shifting the longitudinal gauge boson and the scalar masses obtained by considering only the first two terms in the effective potential [19]. This shift in the thermal masses of longitudinal gauge bosons and not their transverse parts tends to reduce the strength of the phase transition. The integrals (11) is often estimated in the high temperature approximation, however, in order to take into account the effect of all the (heavy and light) degrees of freedom, we evaluate them numerically.

In order to generate a baryon asymmetry at the electroweak scale [20], the anomalous violating $B+L$ interactions should be switched-off inside the nucleated bubbles, which implies the famous condition for a strong first order phase transition [21]

$$v(T_c)/T_c > 1, \tag{12}$$

where T_c is the critical temperature at which the effective potential exhibits two degenerate minima, one at zero and the other at $v(T_c)$. Both T_c and $v(T_c)$ are determined using the full effective potential at finite temperature (9).

In the SM, the ratio $v(T_c)/T_c$ is approximately $\left(2m_W^3 + m_Z^3\right) / \left(\pi v m_h^2\right)$, and therefore the criterion for a strongly first phase transition is not fulfilled for $m_h > 42$ GeV. However, if the one-loop corrections in (13) are sizeable, then this bound could be relaxed in such a way that the Higgs mass is consistent with the measured value at the LHC. This might be possible since the extra charged scalars affect the dynamics of the SM scalar field vev around the critical temperature [22].

In this model, the one loop correction to the Higgs mass due to the charged singlets, when neglecting the Higgs and gauge bosons contributions, is

$$m_h^2 \simeq 2\lambda v^2 + \sum_i \frac{\lambda_i^2 v^2}{16\pi^2} \ln \frac{m_{S_i}^2}{m_t^2}, \tag{13}$$

where the first term on the right hand side of the equation is the Higgs mass at the tree level. If one takes $m_{S_1} = m_{S_2} = 2m_t$ and $\lambda_1 = \lambda_2$, then the Higgs mass is exactly 125 GeV for $\lambda = 10^{-1}$, 10^{-2}, 10^{-3} if $\lambda_1 = 1.82$, 3.68, 3.82, respectively. Note that these values are still within the perturbative regime. On the other hand, these extra corrections could be negative and may relax the large tree-level mass value of the Higgs to its experimental value for λ large. Therefore, it is expected that these extra charged scalars will help the EWPT to be strongly first order by enhancing the value of the effective potential at the wrong vacuum at the critical temperature without suppressing the ratio $v(T_c)/T_c$, and therefore avoiding the severe bound on the mass of the SM Higgs. However, as it has been shown in the previous section, the relic density requires large values for m_{S_1} and so the Higgs mass in Eq. (13) can be easily set to its experimental value (125 GeV),while keeping S_2 light, for small doublet quartic coupling (which gives a strong EWPT). Thus, both the measured values of the Higgs mass and the requirement for the EWPT to be strongly first order are not in conflict with values of m_2 smaller than 245 GeV (as required from the observed relic density).

During the Universe cooling, the Higgs vev decreases slower than the SM case, where it decays quickly to zero just around $T \sim 100$ GeV. Here it is delayed up to TeV due to the existence of the extra charged scalars; and the EWPT occurs around $T \sim 100$ GeV due to the fact that the effective potential at the wrong vacuum ($< h >= 0$) is temperature-dependant through the charged scalars thermal masses in the symmetric phase [9].

In July 2012, ATLAS [23] and CMS [24] collaborations have announced the observation of a scalar particle with mass $\simeq 125$ GeV at about 5 σ confidence level. The question is whether or not this is really the SM Higgs or some Higgs-like state with different properties. Indeed, the fit of the data by the ATLAS collaboration seems to show an excess in $h \to \gamma\gamma$ events by more than 50% with respect to the SM, while the updated CMS analysis is consistent with the SM. Defining $R_{\gamma\gamma}$ and $R_{\gamma Z}$ to be the decay width of $h \to \gamma\gamma$ and $h \to \gamma Z$ respectively, scaled by their expected SM value, we find that

$$R_{\gamma\gamma} = \left| 1 + \frac{v^2}{2} \frac{\frac{\lambda_1}{m_{S_1}^2} A_0\left(\tau_{S_1}\right) + \frac{\lambda_2}{m_{S_2}^2} A_0\left(\tau_{S_2}\right)}{A_1\left(\tau_W\right) + N_c Q_t^2 A_{1/2}\left(\tau_t\right)} \right|^2, \tag{14}$$

$$R_{\gamma Z} = \left| 1 + s_w^2 \frac{v^2}{2} \frac{\frac{\lambda_1}{m_{S_1}^2} A_0\left(\tau_{S_1}, \zeta_{S_1}\right) + \frac{\lambda_2}{m_{S_2}^2} A_0\left(\tau_{S_2}, \zeta_{S_2}\right)}{c_w A_1\left(\tau_W, \zeta_W\right) + \frac{2(1-8s_w^2/3)}{c_w} A_{1/2}\left(\tau_t, \zeta_t\right)} \right| \tag{15}$$

where $\tau_X = m_h^2/4m_X^2$, $\zeta_X = m_Z^2/4m_X^2$, with m_X is the mass of the charged particle X running in the loop, $N_c = 3$ is the color number, Q_t is the electric charge of the top quark in unit of $|e|$, and

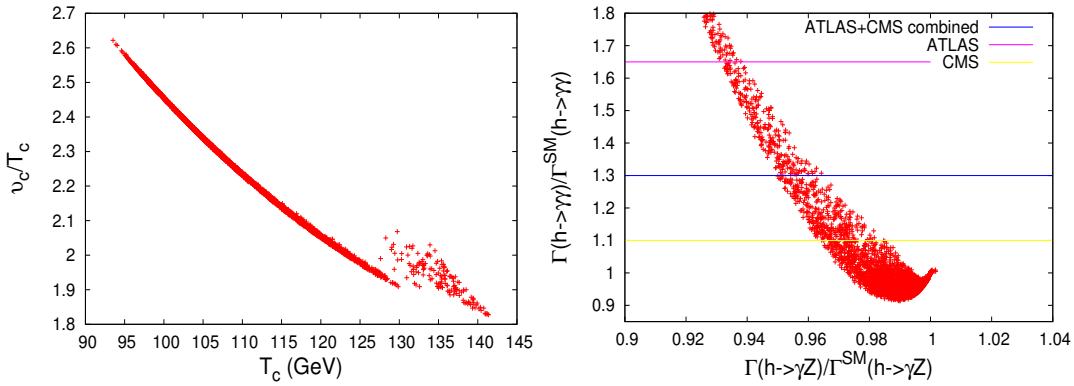

Figure 4. *Left: In the left figure, the critical temperature is presented versus the quantity υ_c/T_c in (12). In the right one, the relative contribution of the one-loop corrections (including the counter-terms) to the Higgs mass versus the parameter λ. Right: The modified Higgs decay rates $B(h \to \gamma\gamma)$ vs $B(h \to \gamma Z)$, scaled by their SM values, due to the extra charged scalars, for randomly chosen sets of parameters. The magenta (yellow) line represents the ATLAS (CMS) recent measurements on the $h \to \gamma\gamma$ channel, while the blue one is their combined result.*

the loop functions A_i are defined in [25]. It is clear that the effect on $B(h \to \gamma\gamma)$ the charged scalar singlets will depend on how light are $S^{\pm}_{1,2}$, the sign and the strength of their couplings to the SM Higgs doublet. For instance, an enhancement can be achieved by taking λ_1 and/or λ_2 to be negative.

In Fig. 4, we present the ratio $\upsilon(T_c)/T_c$ versus the critical temperature T_c (left); and $R_{\gamma\gamma}$ versus $R_{\gamma Z}$ (right) for randomly chosen sets of parameters where the charged scalars are taken to be heavier than 100 GeV, the Higgs mass within the range $124 < m_h < 126$ GeV. In our numerical scan, we take the model parameters relevant for the Higgs decay to be in the range

$$\lambda < 2, \;\; |\lambda_{1,2}| < 3, \;\; m^2_{1,2} < 2 \text{ TeV}^2, \tag{16}$$

where the Higgs mass is calculated at one-loop level. An enhancement of $B(h \to \gamma\gamma)$ can be obtained for a large range of parameter space, whereas $B(h \to \gamma Z)$ is slightly reduced with respect to the SM. It is interesting to note that if one consider the combined ATLAS and CMS di-photon excess, then $R_{\gamma Z}$ is predicted to be smaller than the expected SM value by approximately 5%.

From Fig. 4, we can see that one can have a strongly first order EWPT while the critical temperature lies around 100 GeV without being in conflict with the measured value of the Higgs mass; while $R_{\gamma\gamma}$ can have an enhancement where $R_{\gamma Z}$ remains almost constant.

5. Phenomenology at the ILC

The RH neutrinos do couple to the charged leptons only, then one excepts them to be produced at e^-e^+ colliders, such as the ILC and CLIC with a collision energy $\sqrt{s}$ of few hundreds GeV up to TeV. If a N_iN_k pair is produced inside the collider, they will decay to pairs of charged leptons and N_1N_1, where the charged leptons have not necessary the same flavor. If such decays occur inside the detector, then the signal will be

$$\begin{cases} \not{E} & \text{for} \quad e^+e^- \to N_1N_1 \\ \not{E} + 2\ell_R, & \text{for} \quad e^+e^- \to N_1N_{2,3} \\ \not{E} + 4\ell_R, & \text{for} \quad e^+e^- \to N_{2,3}N_{2,3}, \end{cases}$$

and since $m_{N_i} \geq 100$ GeV, it is very possible that the decay $N_{2,3} \to N_1 + 2\ell_R$ occurs outside the detector, and thus escapes the detection, and therefore considered to be missing energy. The process $e^+e^- \to e^-\mu^+ + \not{E}$ can be a good probe for this model, however there are here so many contributions to the missing energy whose sources both the f's and g's vertices in (1) [26]. Here, we analyze the production of all possible pairs of RH neutrinos, tagged with a photon from an initial state radiation, that is $e^-e^+ \to N_i N_k \gamma$ (with $i,k = 1,2,3$), where one searches for a high p_T gamma balancing the invisible RH neutrinos.

If the emitted photon is soft or collinear, then one can use the soft/collinear factorization form [27]

$$\frac{d\sigma\left(e^+e^- \to N_i N_k \gamma\right)}{dx d\cos\theta} \simeq \mathcal{F}(x,\cos\theta)\hat{\sigma}\left(e^+e^- \to N_i N_k\right), \tag{17}$$

$$\mathcal{F}(x,\cos\theta) = \frac{\alpha_{em}}{\pi}\frac{1+(1-x)^2}{x}\frac{1}{\sin^2\theta}. \tag{18}$$

with $x = 2E_\gamma/\sqrt{s}$, here θ is the angle between the photon and electron and $\hat{\sigma}$ is the cross section evaluated at the reduced center of mass energy $\hat{s} = (1-x)s$. Collinear photon with the incident electron or positron could be a good positive signal, especially if the enhancement in (17) is more significant than the SM background.

There are two leading SM background processes: a) the neutrino counting process $e^-e^+ \to \nu_i\bar{\nu}_i\gamma$ from the t-channel W exchange and the s-channel Z exchange, and b) the Bhabha scattering with an extra photon $e^-e^+ \to e^-e^+\gamma$, which can mimic the N_iN_i signature when the accompanying electrons or photons leave the detector through the beam pipe [28]. In addition to putting the cut on the energy of the emitted photon, one can reduce further the mono-photon neutrino background, by polarizing the incident electron and positron beams such that

$$\frac{N_{e^-_R} - N_{e^-_L}}{N_{e^-_R} + N_{e^-_L}} >> 50\%; \qquad \frac{N_{e^+_R} - N_{e^+_L}}{N_{e^+_R} + N_{e^+_L}} << 50\%, \tag{19}$$

where $N_{e^-_{L,R}}$ and $N_{e^+_{L,R}}$ are the number densities of the left (right)-handed electrons and positrons per unit time in the beam. At $\sqrt{s} >> 100$ GeV the process $e^-e^+ \to \nu_i\bar{\nu}_i\gamma$ is dominated by the W-exchange, and hence one expect that having the electron (positron) beam composed mostly of polarized right handed (left handed) electrons (positron) reduces this background substantially, whereas the signal increases since N_i couples to the right handed electrons.

When estimating the total cross section $\sigma\left(e^+e^- \to N_iN_k\right)$ [9], we can present the differential cross section versus the photon energy for two values of collision energies $\sqrt{s} = 500$ GeV and 1 TeV; using the approximation (17), by integrating over the angle θ taking into account the minimum value of electromagnetic calorimeter acceptance in the ILC to be $\sin\theta > 0.1$ [29].

We see that for the benchmark shown in Fig. 5, the heaviest RH neutrino is largely produced due to its large couplings to the electron/positron. Thus, for this particular benchmark the missing energy is dominated not by the DM, but rather by the other RH neutrinos. Another interesting process that might be possible to search for at both lepton and hadron colliders is the production of $S^\pm_{1,2}$. At the LHC they can be pair produced in an equal number via the Drell-Yan process, with a production rate of $S^\pm_{1,2}$ that is suppressed at very high energies, and so we expect that most of the produced $S^\pm_{1,2}$ will have energies not too far from their masses. Then, each pair of charged scalars decays into charged leptons and missing energy, such as e^+e^-, $\mu^+\mu^-$, μ^+e^-. The observation of an electron (positron) and anti-muon (muon), will be a strong signal for the production of the charged scalars of this model. The energy carried out by the charged leptons, $\ell^+_\alpha\ell^-_\beta$, produced in the decay of $S^\pm_{1,2}$ will be limited by the phase space available to N_1 and $\ell_{\alpha,\beta}$ since $m_{S_2} - m_{N_1} << m_{S_2}$. On the other hand, the leptons originating from the decay

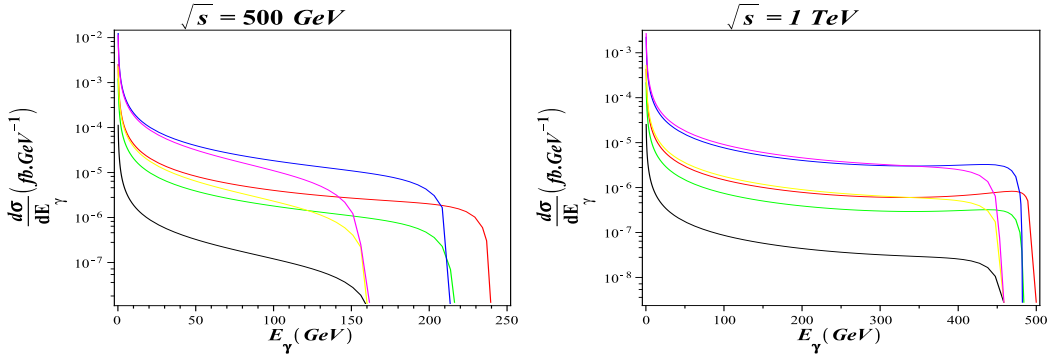

Figure 5. *The photon spectra from the processes* $e^+e^- \to N_iN_k\gamma$ *where the curves: red, green, black, blue, yellow, magenta correspond to (i,k)=(1,1), (1,2), (2,2), (1,3), (2,3), (3,3) respectively. Here, we considered the following favored mass values:* $m_{N_1} = 52.53$ *GeV,* $m_{N_2} = 121.80$ *GeV,* $m_{N_3} = 126.19$ *GeV,* $m_{S_2} = 144.28$ *GeV, and the coupling values:* $g_{1e} = -4.19 \times 10^{-2}$, $g_{2e} = 2.10 \times 10^{-2}$ *and* $g_{3e} = -6.75 \times 10^{-2}$.

of $S_1^\pm$ will be produced in association with a SM neutrino, and hence can have energy as large as $\sim m_{S_1}$. Thus, by putting the appropriate energy cuts on the energy of final states $e^\pm\mu^\mp$ and discriminating the SM background (from the decay of $pp \to W^+W^- + X \to \ell_\alpha\ell_\beta + \nu's$), one can, in principle, identify the signal for the charged scalars. This requires a detailed a analysis which we plan to carry out in a future publication [26].

6. Conclusion

In this paper, we analyzed a radiative model for neutrino masses, generated at three loop level. Beside it can accommodate the neutrino oscillation data and be consistent with the LFV processes, it provides a DM candidate with a mass lying between few GeV up to 225 GeV; and a relatively light charged scalar, $S_2^\pm$, with a mass below 245 GeV. Furthermore, we showed that the charged scalar singlets can give an enhancement for $B\,(h \to \gamma\gamma)$, whereas the decay $B\,(h \to \gamma Z)$ get a small suppression, compared to the SM. We also found that charged scalars with masses close the electroweak scale make the electroweak phase transition strongly first order. Since N_1 couples only to leptons, it can not be observed in experiments for direct dark matter searches. However it might be possible to search for such particle in indirect detection experiments, such as Fermi-LAT, and at future linear colliders, such as the international linear collider (ILC). Thus, for this particular benchmark the missing energy is dominated not by the DM, but rather by the other RH neutrinos.

Acknowledgments: This work is supported by the Algerian Ministry of Higher Education and Scientific Research under the PNR '*Particle Physics/Cosmology: the interface*', and the CNEPRU Project No. *D01720130042*.

[1] P. Minkowski, Phys. Lett. B 67 (1977) 421; M. Gell-Mann, P. Ramond and R. Slansky, Proceedings of the Supergravity Stony Brook Workshop, New York 1979, eds. P. Van Nieuwenhuizen and D. Freedman; T. Yanagida, Proceedings of the Workshop on Unified Theories and Baryon Number in the Universe, Tsukuba, Japan 1979, eds. A. Sawada and A. Sugamoto; R. N. Mohapatra and G. Senjanovic, Phys. Rev. Lett. 44 (1980) 912; J. Schechter and J.W.F. Valle, Phys. Rev. D 22 (1980) 2227.

[2] M. Fukugita and T. Yanagida, Phys. Lett. B 174 (1986) 45.

[3] A. Zee, Phys. Lett. B 161 (1985) 141.

[4] X.-G. He, Eur. Phys. J. C 34 (2004) 371; P.H. Frampton, M.C. Oh and T. Yoshikawa, Phys. Rev. D 65 (2002) 073014.

[5] K.S. Babu, Phys. Lett. B 203 (1988) 132.

[6] L.M. Krauss, S. Nasri and M. Trodden, Phys. Rev. D 67 (2003) 085002.
[7] M. Aoki, S. Kanemura and O. Seto, Phys. Rev. Lett. 102 (2009) 051805; Phys. Rev. D 80 (2009) 033007; M. Aoki, S. Kanemura, K. Yagyu, Phys. Rev. D 83 (2011) 075016; M. Gustafsson, J.M. No and M.A. Rivera, Phys. Rev. Lett. 110 (2013) 211802.
[8] K. Cheung and O. Seto, Phys. Rev. D 69 (2004) 113009.
[9] A. Ahriche and S. Nasri, JCAP 07 (2013) 035.
[10] J. Adam et al. [MEG Collaboration], arXiv:1303.0754 [hep-ex].
[11] J. Beringer et al. (Particle Data Group), Phys. Rev. D 86 (2012) 010001.
[12] G. Aad et al. (ATLAS Collaboration), Phys. Lett. B 716 (2012) 1.
[13] S. Chatrchyan et al. (CMS Collaboration), Phys. Lett. B 716 (2012) 30.
[14] B. Pontecorvo, Sov. Phys. JETP 26 (1968) 984; Z. Maki, M. Nakagawa and S. Sakata, Prog. Theor. Phys. 28 (1962) 870.
[15] D.V. Forero, M. Tortola and J.W.F. Valle, Phys. Rev. D 86 (2012) 073012.
[16] F. Simkovic, A. Faessler, H. Muther, V. Rodin and M. Stauf, Phys. Rev. C 79 (2009) 055501.
[17] P.A.R. Ade et al. [Planck Collaboration], arXiv:1303.5062 [astro-ph.CO].
[18] L. Dolan and R. Jackiw, Phys. Rev. D 9 (1974) 3320; S. Weinberg, Phys. Rev. D 9 (1974) 3357.
[19] M.E. Carrington, Phys. Rev. D 45 (1992) 2933.
[20] V. Kuzmin, V. Rubakov and M.E. Shaposhnikov, Phys. Lett. B 155 (1985) 36.
[21] M.E. Shaposhnikov, Nucl. Phys. B 287 (1987) 757; ibid 299 (1988) 797.
[22] A. Ahriche, Phys. Rev. D 75 (2007) 083522; A. Ahriche and S. Nasri, Phys. Rev. D 83 (2011) 045032; Phys. Rev. D 85 (2012) 093007.
[23] ATLAS Collaboration, Report No. ATLAS-CONF-2013-014, March 2013.
[24] C. Ochando [CMS Collaboration], Talk presented at Rencontres de Moriond, La Thuile, Italy, 9-16, March 2013.
[25] A. Djouadi, Phys. Rept. 457 (2008) 1.
[26] A. Ahriche, S. Nasri and R. Soualah, in preparation.
[27] A. Birkedal, K. Matchev and M. Perelstein, Phys. Rev. D 70 (2004) 077701.
[28] C. Bartels, M. Berggren and J. List, Eur. Phys. J. C 72 (2012) 2213.
[29] J.A. Aguilar-Saavedra et al. [ECFA/DESY LC Physics Working Group Collaboration], hep-ph/0106315.